ISSN 0031-918X, Physics of Metals and Metallography, 2017, Vol. 118, No. 2, pp. 150–157. © Pleiades Publishing, Ltd., 2017.
Original Russian Text © V.V. Ovchinnikov, F.F. Makhin'ko, N.V. Gushchina, A.V. Stepanov, A.I. Medvedev, Yu.N. Starodubtsev, V.A. Kataev, V.S. Tsepelev, V.Ya. Belozerov, 2017, published in Fizika Metallov i Metallovedenie, 2017, Vol. 118, No. 2, pp. 158–166.

STRUCTURE, PHASE TRANSFORMATIONS, AND DIFFUSION

Effect of Ion Irradiation on the Nanocrystallization and Magnetic Properties of Soft Magnetic $Fe_{72.5}Cu_1Nb_2Mo_{1.5}Si_{14}B_9$ Alloy

V. V. Ovchinnikov[a, b, *], F. F. Makhin'ko[a], N. V. Gushchina[a], A. V. Stepanov[a], A. I. Medvedev[a, b], Yu. N. Starodubtsev[b, c], V. A. Kataev[a, b], V. S. Tsepelev[a, b], and V. Ya. Belozerov[c]

[a] *Institute of Electrophysics, Ural Branch, Russian Academy of Sciences, ul. Amundsena 106, Ekaterinburg, 620016 Russia*
[b] *Yeltsin Ural Federal University, ul. Mira 19, Ekaterinburg, 620002 Russia*
[c] *Scientific Production Association GammaMet, ul. Kirova 28, Ekaterinburg, 620028 Russia*
**e-mail: viae05@rambler.ru*

Received August 15, 2016; in final form, September 16, 2016

Abstract—The effect of accelerated Ar^+ ions on the crystallization process and magnetic properties of nanocrystalline $Fe_{72.5}Cu_1Nb_2Mo_{1.5}Si_{14}B_9$ alloy has been studied using X-ray diffraction analysis, transmission electron microscopy, thermomagnetic analysis, and other magnetic methods. Irradiation by Ar^+ ions with an energy of 30 keV and a fluence of 3.75×10^{15} cm^{-2} at short-term heating to a temperature of 620 K (which is 150 K below the thermal threshold of crystallization) leads to the complete crystallization of amorphous alloy, which is accompanied by the precipitation of the α-Fe(Si) solid solution crystals (close in composition to $Fe_{80}Si_{20}$), Fe_3Si stable phase, and metastable hexagonal phases. The crystallization caused by irradiation leads to an increase in the grain size and changes the morphology of grain boundaries and volume fraction of crystalline phases, which is accompanied by changes in the magnetic properties.

Keywords: ion irradiation, soft magnetic alloy, crystallization, nanocrystalline structure, X-ray diffraction, transmission electron microscopy, magnetic methods of analysis

DOI: 10.1134/S0031918X17020107

INTRODUCTION

At present, soft magnetic nanocrystalline materials are manufactured in commercial quantities. Nevertheless, these materials are not completely studied and, on the contrary, up to now, nanocrystalline electrotechnical alloys are of substantial interest as objects for physical research. The alloys under consideration contain elements, which favor the formation of amorphous structure in ribbons 20–25 μm thick during rapid quenching from the melt. Alloys that have undergone nanocrystallization contain elements that assure the formation of nanosized grains during crystallization of an amorphous precursor. The classic soft magnetic nanocrystalline FINEMET alloy, the composition of which is $Fe_{73.5}Cu_1Nb_3Si_{13.5}B_9$, meets all the aforementioned requirements. Its components, such as Si and B, ensure the formation of amorphous precursor; Cu and Nd allow one to obtain crystallites no more than 20 nm in size after heat treatment [1]. The average nanograin size is about 10 nm; the chemical composition of nanograins corresponds to the α-Fe(Si) solid solution, which allows the coercive force to be decreased by several orders of magnitude, i.e., to a value of 1 A/m [2–4].

To reach the required magnetic properties, FINEMETs are subjected to heat treatment in a vacuum (or in a protective atmosphere). The partial substitution of Mo for Nb allows one to design the $Fe_{72.5}Cu_1Nb_2Mo_{1.5}Si_{14}B_9$ alloy, the high magnetic permeability of which is achieved by heat treatment in air [5, 6]. Subsequent studies showed that the substitution of Mo for Nb decreases the activation energy of nanocrystallization and increases the fraction of crystalline phase in the alloy [7, 8].

Modern applications of soft magnetic materials and, therefore, the range of required combinations of properties (such as the coercive force, saturation magnetization, and hysteresis loop shape and others) are constantly widening. Therefore, the necessity to develop efficient methods of controlling the properties of electrotechnical alloys increases. Recent studies have indicated that ion-beam treatments show promise as the method of controlling the properties of alloys. At the same time, it is safe to say that processes taking place in soft magnetic materials in the course of exposing them to accelerated ion beams are still poorly understood.

The majority of studies related to the problem are based on the intuitive assumption that changes in the structure and properties of objects exposed to irradiation are limited only by ion-penetration zone and its nearest vicinity. In particular, it was found in [9, 10]

that the irradiation of the $Fe_{76}Mo_8Cu_1B_{15}$ and $Fe_{74}Nb_3Cu_1Si_{16}B_6$ alloys by the ions N^+ with energies of 110–130 keV affects the chemical short-range order at the irradiated surface to a depth of to 200 nm. Under irradiation conditions used in [9, 10], no changes at the unirradiated side of ribbon were found.

First, studies indicating the existence of structural changes in materials were performed by authors in [11–20]. The substantial effect of ion-beam treatment on the magnetic properties of the $Fe_{69}Ni_{31}$ alloy was found in [11–14]; the analogous effect on the atomic and the magnetic structure and electrotechnical properties of electrical steel strips (to 0.35 mm in thickness), as well as of the permalloy, amorphous and nanocrystalline ribbons made of soft magnetic materials, was found in [15–18].

The substantial effect of irradiation with N^+ and Ar^+ ions, which was performed in continuous and pulsed-periodic modes (the effect is different for different irradiation conditions), on the hyperfine magnetic structure of Mössbauer spectrum of the $Fe_{69}Ni_{31}$ alloy was shown in [11–14]. This effect is explained by the accelerated redistribution of atoms and the formation of short-range atomic order in the volume of foils 30 μm thick during ion irradiation with heating, which is insufficient for the occurrence of diffusion processes. The analogous changes of hyperfine magnetic fields at atomic nuclei of the alloy were previously only observed under conditions of ultrahigh pressure, whereas traditional heating to 200°C does not change the shape of the spectrum.

Taking into account the damaging (the formation of defects in the surface layer to several tens of nanometers in thickness) and radiation dynamic (shock-wave action at a multiple depth) effects of ions [20], irradiation conditions for 3424 anisotropic electrical steel (Fe–3 wt % Si) were optimized in [16] in order to form the specific atomic [15], defect, and magnetic domain structures (the domain structure is substantially finer than the initial domain structure). This irradiation treatment (by Ar^+ ions with the energy $E =$ 20 keV; the ion current density is $j = 50$–100 μA/cm^2 and the fluence is $(1–2) \times 10^{16}$ cm^{-2}) allowed the authors to decrease the magnetization reversal losses at operating frequencies of 400–5000 Hz and an induction of 1.5 T from 6 to 20%. The depth of changes in the magnetic structure (to 5–10 μm) exceeds projective ranges of accelerated Ar^+ ions by several orders of magnitude.

The improvement of magnetic properties of the anisotropic electric steel results from the complex combination of various causes, such as the increase in the degree of atomic structure perfectness at the expense of more complete ordering during irradiation annealing [16], the formation of a specific multilayer domain structure that consists of narrow domains perpendicular to the direction of easy magnetization ([001]), etc.

A detailed study of the effect of conditions of irradiation treatment on the magnetic properties of $Fe_{73.5}Cu_1Nb_3Si_{13.5}B_9$ amorphous ribbons with accelerated Ar^+ ion beams was performed in [17, 18]; the irradiation treatment was performed after the standard finished heat treatment that ensures the formation of the nanocrystalline structure and the best properties of the ribbons (annealing at 530°C for 0.5 h). As a result, the optimum irradiation conditions were determined, which allowed the authors to additionally decrease the magnetization reversal losses by an average of 10% at frequencies of 50–10000 Hz at the expense of the formation of a perfect structure.

A method of combined ion-beam and thermomagnetic treatment of permalloy (Fe–70 wt % Ni) and transformer steel (Fe–3 wt % Si) was patented [19]. The irradiation dynamic action of accelerated-ion beam, which is realized before the thermomagnetic treatment, leads to the deep refining of the structure of these materials with respect to impurities and defects [18] and, therefore, to the improvement of magnetic properties. The decrease in the coercive force (compared to the level achieved by only thermomagnetic treatment) for permalloy is 27%. The additional decrease in the magnetization reversal losses at the expense of combined treatment of anisotropic electric steel is about 15%.

X-ray diffraction analysis was used in [21] to study the effect of irradiation by Ar^+ ions with an energy of $E = 30$ keV at an ion current density $j = 50$ μA/cm^2 and a fluence of 1.5×10^{18} cm^{-2} on the crystallization of Co-based amorphous alloys. It has been shown that, after irradiation, the temperature of the onset of crystallization decreases by 200–300 K, and new crystalline phases appear that are not formed during traditional temperature-induced crystallization. The thickness of studied layer was 6.2 μm, which substantially exceeds the projective ranges of accelerated Ar^+ ions in the aforementioned alloys.

The effect of the ion-irradiation-induced decrease in the crystallization temperature was observed previously for pure copper plates subjected to severe plastic deformation [22]. The analogous effect was observed for molybdenum [23]. Thus, ion-beam irradiation can improve the atomic and the magnetic structure of alloys. Under certain conditions, due to the irradiation dynamic action of the ion beam [20], which is related to the propagation of postcascade powerful elastic and shock waves, the depth of the magnetic domain structure changes and, as was shown above, exceeds the projective ranges of Ar^+ ions by several orders of magnitude [16]. In this case, the result of the action is determined by both ion beam parameters and, to a large degree, by the initial state of material.

In the present study, we investigated the effect of irradiation by Ar ions with an energy of 30 keV on the nanocrystallization process and magnetic properties of soft magnetic $Fe_{72.5}Cu_1Nb_2Mo_{1.5}Si_{14}B_9$ alloy.

EXPERIMENTAL

The $Fe_{72.5}Cu_1Nb_2Mo_{1.5}Si_{14}B_9$ alloy was melted using a vacuum induction furnace. An amorphous ribbon 25 μm in thickness and 10 mm in width was prepared by rapid quenching from the melt (in the form of plane jet). Ribbon samples were subjected to irradiation with continuous Ar^+ ion beams with an energy of 30 keV using an ILM-1 implanter equipped with a PUL'SAR-1M ion source based on cold hollow-cathode glow discharge [24], which allows one to operate in both continuous and pulse-periodic modes. Continuous ion beams of round cross section ($S > 100$ cm^2) characterized by constant ion current density over the beam cross section were used. A collimator was used to cut from the round-section Ar^+ ion beam a 2×10-cm^2 section of a stripwise ion beam; a specific device and vacuum chamber were used to move alloy ribbons above the ribbon beam at a rate of 1 cm/s. The density of the ion current was $j = 300$ μA/cm^2 and the irradiation dose (fluence) was $D = 3.75 \times 10^{15}$ cm^{-2}. In the case of this fluence, each point of the moved ribbon was exposed to the beam for ~2 s. To monitor the temperature of the ribbon sample, a thin chromel–alumel thermocouple was used, which was connected to an Adam 4000 (Advantech) automated digital-signal registration system. In the course of irradiation, samples (moved ribbons) were briefly heated with an ion beam (within the irradiation zone) to 350 ± 10°C (~620 K). The initial and irradiated samples, namely, flat ribbons and ribbons turned in the form of rings 24 mm in inner diameter and 23 mm in outer diameter were annealed in air at temperatures of 730–840 K for 1 h. To obtain reproducible data on the structure and properties, three samples were simultaneously irradiated under the aforementioned conditions. Other pilot irradiation conditions were also used, based on which the aforementioned regime was selected and realized.

X-ray diffraction patterns were taken using a D8 DISCOVER diffractometer (Germany, Bruker), Cu $K_{\alpha 1,2}$ radiation, Bragg–Brentano focusing geometry, and a graphite monochromator mounted at the diffracted beam. Data were processed using TOPAS 3 full-profile fitting software. The volume fraction of amorphous component was estimated taking into account the contribution of two diffuse maxima. We used the Scherrer method (and the width at half-height of diffraction maximum) to estimate the average size of crystallites; the shape correction factor was 0.89. No substantial differences were found in X-ray diffraction patterns taken from irradiated and unirradiated sides of sample. This fact confirms the available data on the long-range effect of accelerated ions on metastable media [12–20]; the studied amorphous ribbons prepared by rapid quenching are among them.

The structural state of samples was studied by transmission electron microscopy using a JEM 200CX microscope. Data for estimating the average grain size and grain-size distribution histograms were obtained in analyzing dark-field images of 400–450 grains. The temperatures of magnetic and structural transitions were determined by thermomagnetic analysis. The magnetic properties were measured using ring samples and the magnetic measuring system, the performance of which is based on the realization of the induction pulse method.

RESULTS AND DISCUSSION

Figure 1 shows X-ray diffraction patterns for (a) as-quenched ribbons and (b) samples subjected to heat treatment at 800 K for 1 h, as well as for (c) as-quenched ribbon irradiated with Ar^+ ions and (d) this very ribbon, but additionally subjected to subsequent heat treatment under the same conditions. The X-ray diffraction pattern of the unirradiated (as-quenched) ribbon indicates only a halo related to the amorphous structure (Fig. 1a). After the heat treatment of the ribbon at temperatures above 750 K, the reflections of crystalline phases, along with the halo, appear in the X-ray diffraction patterns. In this case, as the temperature increases, the center of halo tends to shift to the low angle range.

Figure 1b shows the X-ray diffraction pattern for the unirradiated sample subjected to heat treatment at 840 K for 1 h. An analysis showed that the α-Fe-based solid solution is one of the formed crystalline phases; the silicon content in the solid solution was estimated using the crystal lattice parameter. The determined lattice parameter equal to 0.2845 nm corresponds to a composition of $Fe_{80}Si_{20}$. The other crystalline phase is the Fe_3Si compound with a lattice parameter equal to 0.5670 nm.

The noticeable fraction of the crystalline phase appears in unirradiated samples only at a temperature of 770 K. At the same time, the crystallization over the entire volume of ribbon takes place during irradiation resulting in short-time heating to 620 K (the bottom temperature of irradiation-induced crystallization was not determined). Figure 2 shows the dependence of the volume fractions of the (*1*) amorphous and (*2*) crystalline phases, (*3*) $Fe_{80}Si_{20}$ solid solution, and (*4*) stable Fe_3Si phase and (*5*) the initial magnetic permeability μ on the annealing temperature (T_{ann}). The initial relative magnetic permeability of as-quenched amorphous ribbon is 950. After heat treatment at temperatures of 730–790 K, the magnetic permeability increases to 20000. At these temperatures, the structure of the ribbon is characterized by a dominant amorphous phase; the increase in the magnetic permeability is related to the relaxation of internal stresses induced in the ribbon by melt quenching. The increase in the volume fraction of crystalline phase at temperatures above 790 K correlates with the increase in the magnetic permeability of alloy. It should be noted that, over the temperature range under study, the vol-

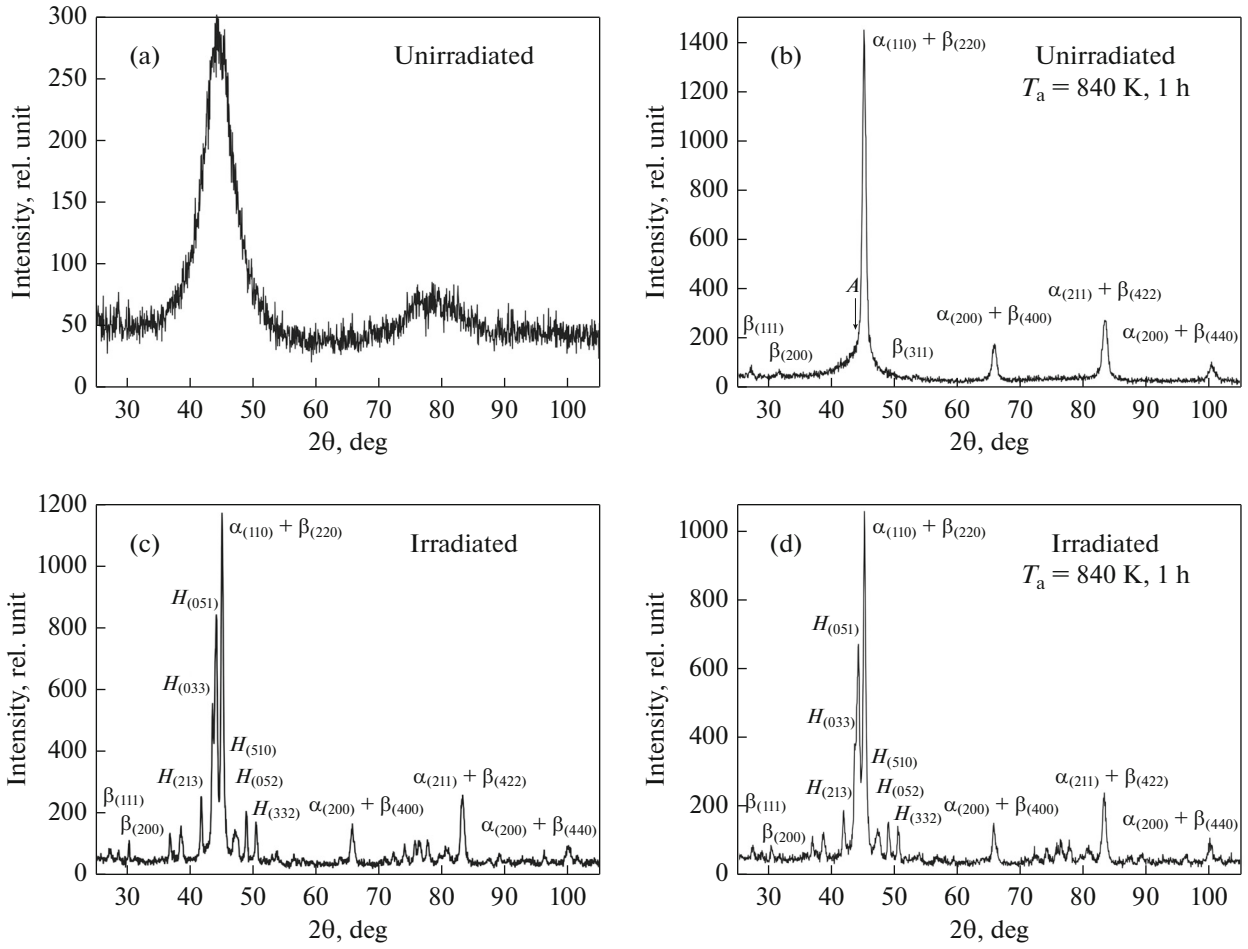

Fig. 1. X-ray diffraction patterns for the $Fe_{72.5}Cu_1Nb_2Mo_{1.5}Si_{14}B_9$ ribbon (a) in the as-quenched state, (b) after subsequent heat treatment at 840 K for 1 h, (c) after irradiation ($\tau_{irr} \sim 2$ s) with Ar^+ ions, and (d) subsequent heat treatment at 840 K for 1 h; reflections of the amorphous phase (*A*), hexagonal phase (*H*), αFe(Si) solid solution (α), and cubic Fe_3Si phase (β) are indexed.

ume fraction of the $Fe_{80}Si_{20}$ solid solution exceeds that of the ordered Fe_3Si phase.

After the irradiation of samples by Ar^+ ions with an energy of 30 keV, during which the temperature for a short-time (2 s) reached ~620 K (that is 150 K below the temperature of the onset of temperature-induced crystallization), the crystallization of the samples was observed. No halo is observed in the X-ray diffraction pattern; diffraction reflections correspond to a multiphase crystalline structure (Fig. 1c). The heat treatment of the irradiated sample at 840 K for 1 h hardly changes the X-ray diffraction pattern (Fig. 1d). The analysis shows that some reflections correspond to crystalline phases that are analogous to those observed above, namely, to the α-Fe(Si) solid solution and Fe_3Si. Moreover, the X-ray diffraction pattern indicates the presence of an *H* phase with a hexagonal structure (space group $P6_3/mmc$), which was identified in [25] in studying late crystallization stages of FINEMET alloy and its crystallization after laser irradiation. We failed to describe the observed X-ray dif-

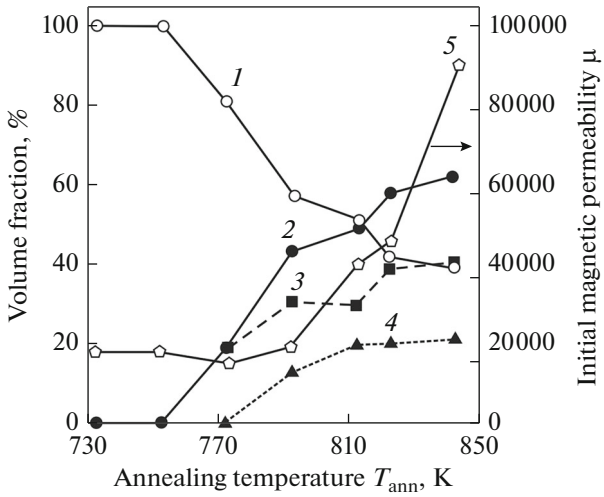

Fig. 2. Dependences of the volume fractions of (*1*) amorphous and (*2*) crystalline phases and separately of (*3*) $Fe_{80}Si_{20}$ solid solution and (*4*) Fe_3Si and (*5*) of the initial magnetic permeability (μ) on the annealing temperature (T_{ann}) for the unirradiated $Fe_{72.5}Cu_1Nb_2Mo_{1.5}Si_{14}B_9$ ribbon.

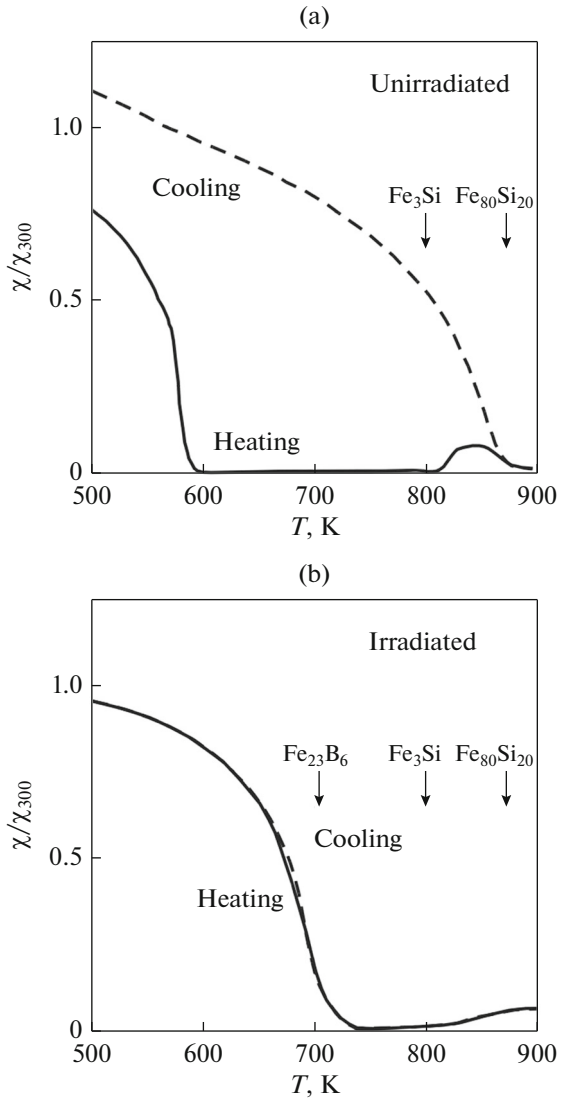

Fig. 3. Temperature dependences of relative magnetic susceptibility (χ/χ_{300}) of (a) unirradiated and (b) irradiated $Fe_{72.5}Cu_1Nb_2Mo_{1.5}Si_{14}B_9$ ribbon; Curie temperatures of crystalline phases are shown.

fraction pattern using well-known crystalline structures, such as Fe_3Si, αFe(Si), FeSi (all are cubic), $FeSi_2$ (orthorhombic or tetragonal), Fe_5Si_3 (hexagonal), $Fe_{11}Si_5$ (cubic), $Fe_{23}B_6$ (cubic), and Fe_2B (tetragonal). Based on this fact, we conclude that either a number of intense reflections are absent in the X-ray diffraction pattern or the set of observed reflections does not correspond to these structures. No substantial changes are observed in changing occupations of lattice sites and adding preferred orientations. Along with the Fe_3Si and αFe(Si) phases, phases similar to the $Fe_{23}B_6$, Fe_5Si_3, and Fe_2B ones are likely to be present in the material.

Data given in the table indicate the decrease in the volume fraction of the Fe_3Si crystalline phase and increase in the volume fraction of the α-Fe(Si) solid solution with increasing annealing temperature, i.e., with increasing the volume fraction of crystalline phase with the low silicon content. This agrees with data of [26], which has proved the decrease in the silicon content in the crystalline phase at late crystallization stages. The fraction of hexagonal *H* phase slightly varies in the course of annealing. As the annealing temperature increases, the magnetic permeability increases and, at 840 K, it reaches 11 600.

Figure 3 shows the results of a thermomagnetic analysis of as-quenched (a) unirradiated and (b) irradiated samples. Arrows show the Curie temperatures of the crystalline phases precipitated during the crystallization of FINEMET alloy [27–29]. The abrupt decrease in the magnetic susceptibility during heating to 587 K corresponds to the Curie temperature of the $Fe_{72.5}Cu_1Nb_2Mo_{1.5}Si_{14}B_9$ alloy in the amorphous state. The increase in the magnetic susceptibility at 807 K is related to the appearance of ferromagnetic α-Fe(Si) solid crystallites [1]. The maximum magnetic susceptibility corresponds to 840 K. We assume that this temperature corresponds to the alloy state characterized by the maximum volume of crystalline phase. The further decrease in the magnetic susceptibility is caused by disordering thermal effect on the ferromagnetic ordering. A temperature of 879 K, at which the relative magnetic susceptibility approaches zero, is close to the Curie temperature of the $Fe_{80}Si_{20}$ solid solution [27]. The temperature dependence of the magnetic susceptibility during cooling closely corresponds to that for $Fe_{80}Si_{20}$ solid solution crystallites.

The reversibility of the thermomagnetic curve measured for the irradiated sample (Fig. 3b) indicates the weak effect of the temperature on the crystalline structure formed during irradiation. The thermomag-

Initial magnetic permeability (μ), volume fraction (*V*) of phases, and crystal lattice parameters (*a* and *c*) for irradiated samples subjected to heat treatment at T_{ann} for 1 h

T_{ann}, K	μ	α-Fe(Si)		Fe_3Si		*H* phase	
		V, %	*a*, nm	*V*, %	*a*, nm	*V*, %	*a*/*c*, nm
300	1000	44	0.2848	30	0.5678	26	1.2291/0.7695
750	5000	47	0.2846	22	0.5682	31	1.2295/0.7694
790	5200	55	0.2845	12	0.5702	33	1.2301/0.7699
840	11600	58	0.2844	12	0.5696	30	1.2302/0.7695

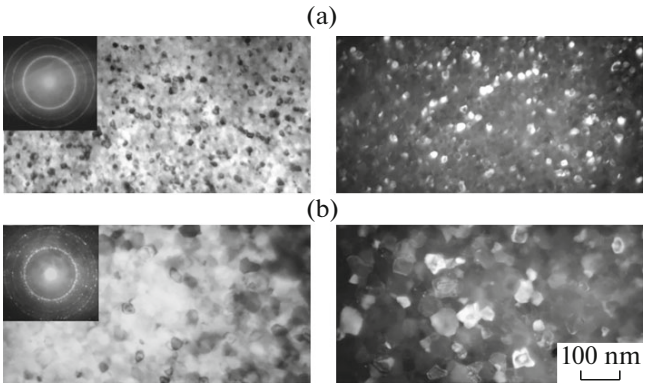

Fig. 4. Structure of (a) unirradiated and (b) irradiated samples subjected to heat treatment at 840 K for 1 h; left and right micrographs are bright-images with electron diffraction patterns and dark-field images taken in 110_α reflection, respectively.

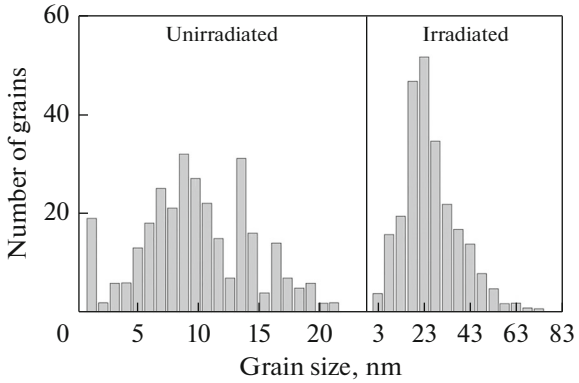

Fig. 5. Grain-size distribution histograms for (a) unirradiated sample subjected to heat treatment at 840 K for 1 h and (b) irradiated sample.

netic curve exhibits no bends that allow one to find ferromagnetic phases with substantially different Curie temperatures. The main phase or group of phases formed after irradiation is characterized by a Curie temperature of 710 K. Among the available phases, the $Fe_{23}B_6$ cubic phase has a close Curie temperature. The Curie temperature of the Fe_5Si_3 phase is 378 K, i.e., it is substantially lower [30].

Figure 4 shows the structure of (a) unirradiated and (b) irradiated samples subjected to heat treatment at 840 K for 1 h. The bright-field image with electron diffraction pattern and dark-field image taken in 110_α reflections show the structure.

Figure 5 shows grain-size distribution histograms. In the unirradiated sample, grains 11 nm in average size are equiaxed. The first and second maxima in the histogram correspond to areas 9 and 14 nm in size, respectively. The average grain sizes of the α-Fe(Si) solid solution and Fe_3Si phase, which were estimated by Scherrer method, are 17 and 19 nm, respectively.

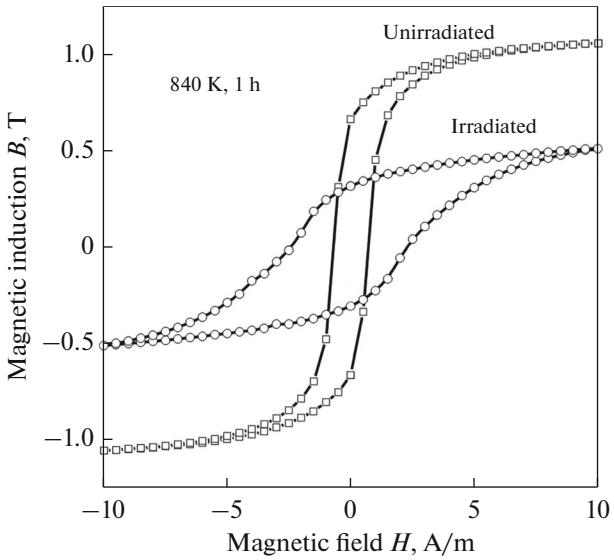

Fig. 6. Minor magnetic hysteresis loops at H_{max} = 10 A/m for unirradiated and irradiated samples subjected to heat treatment at 840 K for 1 h.

After irradiation, the grain size substantially increases and grain shape changes. The grain shape becomes intricate, and grain boundaries become wider. The average grain size is 25 nm. The average grain sizes of the α-Fe(Si) solid solution, Fe_3Si, and *H* phase, which were estimated by Scherrer method, are 21, 30, and 27 nm, respectively.

Changes in the structure and phase composition of samples subjected to aforementioned irradiation treatments lead to noticeable changes of the magnetic properties. Figure 6 shows minor magnetic hysteresis loops at H_{max} = 10 A/m for the samples subjected to heat treatment at 840 K for 1 h in the (a) unirradiated and (b) irradiated state. After irradiation, the magnetic induction in a field of 10 A/m decreases by more than 50% and the coercive force increases from 0.70 to 2.4 A/m. The initial and maximum magnetic permeability decrease from 90 000 to 11600 and from 450000 to 52000, respectively.

The performed test studies of the effect of ion-beam treatment and varied irradiation conditions on the structure and properties of alloy have showed the high sensitivity of magnetic properties to the irradiation conditions. In particular, in principal, this allows the magnetization reversal losses to be decreased; the analogous decrease was studied in [16, 17, 19]. However, extensive evidence is necessary to choose the required irradiation conditions based on statistically reliable data. This assumes the stability of a great number of beam parameters, speed of ribbon movement, conditions of heat removal, etc.

CONCLUSIONS

The study of the effect of Ar^+ ion irradiation on the crystallization process and magnetic properties of soft magnetic nanocrystalline $Fe_{72.5}Cu_1Nb_2Mo_{1.5}Si_{14}B_9$ alloy showed that the irradiation by Ar^+ ions with an energy of 30 keV and a fluence of 3.75×10^{15} cm^{-2} leads to the complete crystallization of amorphous alloy when a temperature of 620 K is achieved, which is 150 K below the lower temperature of crystallization. In the course of crystallization, α-Fe(Si) solid-solution crystals, the composition of which is close to $Fe_{80}Si_{20}$, and stable Fe_3Si and metastable hexagonal phase crystals are formed.

The irradiation-induced crystallization is accompanied by grain growth and changes of the morphology of grain boundaries. The heat treatment of irradiated samples leads to a decrease in the volume fraction of the Fe_3Si crystalline phase and increase in the volume fraction of α-Fe(Si) solid solution. It has been shown that the size of Fe_3Si grains is higher than that of α-Fe(Si) solid solution. The average grain size estimated by Scherrer method is slightly higher than that determined by transmission electron microscopy. The aforementioned changes are accompanied by substantial changes of the magnetic properties.

The preliminary studies showed the high sensitivity of magnetic properties to ion-beam irradiation (radiation annealing) conditions. Thus, in principle, there is the possibility to select parameters, such as the ion energy, density of ion current, fluence, speed of ribbon motion, and temperature of process, in order to reach the given electrotechnical characteristics of alloy. The analogous selection was done in [16, 17, 19] in order to decrease the watt losses in electric steels and a FINEMET alloy that has a close composition.

Taking into account the high stability of the alloy state formed during ion irradiation and the high rate of the structural changes that occurred (even for 2 s irradiation), the regularities of structural changes and the variations in magnetic characteristics at low fluence magnitudes call for detailed studies.

ACKNOWLEDGMENTS

The study was supported by the Russian Scientific Foundation (project no. 15-19-10054).

REFERENCES

1. Y. Yoshizawa, S. Oguma, and K. Yamauchi, "New Fe-based soft magnetic alloys composed of ultrafine grain structure," J. Appl. Phys. **64**, 6044–6046 (1988).
2. G. Herzer, "Grain structure and magnetism of nanocrystalline ferromagnets," IEEE Trans. Magn. **25**, 3327–3329 (1989).
3. Y. Yoshizawa, in *Handbook of Advanced Magnetic Materials 4: Properties and Applications,* Ed. by Y. Liu, D. J. Sellmyer and D. Shindo (Springer-Verlag, New York, 2006).
4. G. Herzer, in *Handbook of Magnetic Materials,* Ed. by K. H. J. Buschow (Elsevier, Amsterdam, 1997).
5. Yu. N. Starodubtsev and V. Ya. Belozerov, *Magnetic Properties of Amorphous and Nanocrystalline Alloys* (Ural. Univ., Ekaterinburg, 2002) [in Russian].
6. V. Tsepelev, V. Konashkov, Y. Starodubtsev, V. Belozerov, and D. Gaipishevarov,"Optimum regime of heat treatment of soft magnetic amorphous materials," IEEE Trans. Magn. **48**, 1327–1330 (2012).
7. J. M. Silveyra, E. Illekova, P. Svec, D. Janickovic, A. Rosales-Rivera, and V. J. Cremaschi, "Phase transformations in Mo-doped FINEMETs," Physica A **405**, 2720–2725.
8. J. M. Silveyra, V. J. Cremaschi, D. Janickovic, P. Svec, B. Arcondo, "Structural and magnetic study of Mo-doped FINEMET," J. Magn. Magn. Mater. **323**, 290–296 (2011).
9. M. Migleirini, A. Lancok, and M. Pavlovic, "Ion bombardment of Fe-based amorphous metallic alloys," Hyperfine Interact. **189**, 45–52 (2009).
10. M. Miglierini, A. Lančok, and M. Pavlovič, "CEMS studies of structural modifications of metallic glasses by ion bombardment," Phys. Met. Metallogr. **109**, 469–474 (2010).
11. V. V. Ovchinnikov, "Self-propagating phases transformations in metastable media induced by ion bombardment," in *Proc. 16th Int. Symp. on Discharges and Electrical Insulation in Vacuum* (Moscow, 1994), Proc. SPIE **2259**, 605–610 (1994).
12. Yu. E. Kreindel' and V. V. Ovchinnikov, "Phase transformations of non-thermal nature and effects of long-range interaction upon bombardment of alloys by gas ions," Fiz. Khim. Obrab. Mater., No. 3, 14–20 (1991).
13. Yu. E. Kreindel and V. V. Ovchinnikov, "Structural transformations and long-range effects in alloys caused by gas ion bombardment," Vacuum **42**, 81–83 (1990).
14. V. V. Ovchinnikov, Yu. D. Kogan, N. V. Gavrilov, and A. K. Shtoltz, "The formation of extraordinary magnetic states in an iron–nickel alloy with bcc–fcc transitions induced by ion irradiation," Surf. Coating Technol. **64**, 1–4 (1994).
15. S. N. Borodin, Yu. E. Kreindel', G. A. Mesyats, and V. V. Ovchinnikov, "Effect of re-ordering at accelerated ion bombardment," Pis'ma Zh. Tekh. Fiz. **15**, 87–90 (1989).
16. B. K. Sokolov, V. V. Gubernatorov, Yu. N. Dragoshanskii, A. P. Potapov, V. V. Ovchinnikov, N. V. Gavrilov, B. Yu. Goloborodskii, D. R. Emlin, E. P. Mikhalishcheva, I. S. Mikhailov, and L. V. Oshurko, "Effect of ion-beam treatment on the magnetic properties of soft magnetic materials, " Phys. Met. Metallogr. **89**, 348–357 (2000).
17. Yu. N. Dragoshanskii, V. V. Gubernatorov, B. K. Sokolov, and V. V. Ovchinnikov, "Structural inhomogeneity and magnetic properties of soft magnetic materials," Dokl.-Phys. **47**, 302–304 (2002).
18. V. V. Gubernatorov, T. S. Sycheva, Yu. N. Dragoshanskii, V. V. Ovchinnikov, and V. A. Ivchenko, "The impact of bombardment by accelerated ions on effects related to the thermomagnetic treatment of fer-

romagnetic materials," Dokl. Phys. **51**, 493–495 (2006).

19. V. V. Gubernatorov, Yu. N. Dragoshanskii, V. A. Ivchenko, V. V. Ovchinnikov, and T. S. Sycheva, "Method of thermomagnetic treatment of magnetically soft materials," RF Patent no. 2321644, MPK C21D 1/04 (2006/01), *Byull. Izobr.* 2008, no. 10.
20. V. V. Ovchinnikov, "Radiation-dynamics effects. Potential for producing condensed media with unique properties and structural states," Phys.-Usp. **51**, 955–964 (2008).
21. V. S. Kraposhin, V. S. Khmelevskaya, M. Y. Yazvitsky, and I. A. Antoshina, "Crystallization of Co-based amorphous alloys under the impact of the ion irradiation and recovery of the amorphous phase," J. Non-Cryst. Solids **353**, 3057–3061 (2007).
22. V. V. Ovchinnikov, V. N. Chernoborodov, E. P. Mikhalishcheva, P. Z. Valiev, R. R. Mulyukov, and N. N. Amirkhanov, "The change of grain boundary structure in ultrafine-grained Cu due to ion bombarding," Trans. Mat. Res. Soc. Jpn. B **16**, 1489–1492 (1994).
23. V. V. Ovchinnikov, N. V. Gushchina, T. M. Gapontseva, T. I. Chashchukhina, L. M. Voronova, V. P. Pilyugin, and M. V. Degtyarev, "Optimal deformation and ion irradiation modes for production of a uniform submicrongrain structure in molybdenum," High Press. Res., No. 5, 300–309 (2015).
24. N. V. Gavrilov, G. A. Mesyats, S. P. Nikulin, G. V. Radkovskii, A. Eklind, A. J. Perry, and J. R. Treglio, "A new broad beam gas ion source for industrial applications," J. Vac. Sci. Technol. A **14**, 1050–1055 (1996).
25. I. V. Lyasotskii, N. B. Dyakonova, E. N. Vlasova, D. L. Dyakonov, and M. Yu. Yazvitskii, "Metastable and quasiperiodic phases in rapidly quenched Fe–B–Si–Nb(Cu) alloys," Phys. Status Solidi A **203**, 259–270 (2006).
26. J. M. Borrego, C. F. Conde, and A. Conde, Thermomagnetic Study of Devitrification in Fe–Si–B–Cu–Nb(–*X*) Alloys," Philos. Mag. Lett. **80**, 359–365 (2000).
27. O. Kubaschewski, *Iron-Binary Phase Diagrams* (Springer-Verlag: Berlin, 1982).
28. C. L. Chien, D. Musser, E. M. Gyorgy, R. C. Sherwood, H. S. Chen, F. E. Luborsky, and J. L. Walter, "Magnetic properties of amorphous Fe_xB_{100-x} ($72 \le x \le 86$) and Crystalline Fe_3B," Phys. Rev. B: Solid State **20**, 283–295 (1979).
29. V. A. Barinov, V. I. Voronin, V. T. Surikov, V. A. Kazantsev, V. A. Tsurin, V. V. Fedorenko, and S. I. Novikov, "Structure and magnetic properties of metastable Fe–B phases," Phys. Met. Metallogr. **100**, 456–467 (2005).
30. L. K. Varga, F. Mazaleyrat, J. Kovac, and A. Kakay, "Magnetic properties of rapidly quenched $Fe_{100-x}S_x$ ($15 \le x \le 34$) alloys," Mater. Sci. Eng., A **304–306**, 946–949 (2001).

Translated by N. Kolchugina